

Chapter 11

Applications of Sensing to Precision Irrigation



Yafit Cohen, George Vellidis, Carlos Campillo, Vasileios Liakos, Nitsan Graff, Yehoshua Saranga, John L. Snider, Jaume Casadesús, Sandra Millán, and Maria del Henar Prieto

Abstract Precision irrigation aims at improving productivity and sustainability by addressing spatial as well as temporal variability of soil and crop water status. This chapter presents three case studies from south-eastern USA, Israel and Spain which relate to different attributes of precision irrigation: (1) type of precision: whether it

Yafit Cohen and Nitsan Graff: Introduction and Case Study 11.2

George Vellidis and Vasileios Liakos: Case Study 11.1

Yehoshua Saranga and John L. Snider: Case Study 11.2

Carlos Campillo, Jaume Casadesús, Sandra Millán and Maria del Henar Prieto: Case Study 11.3

Y. Cohen (✉)

Agricultural Engineering Institute, Agricultural Research Organization, Volcani Institute, Rishon LeZion, Israel

e-mail: yafitush@volcani.agri.gov.il

G. Vellidis · V. Liakos · J. L. Snider

Crop and Soil Sciences Department, University of Georgia, Athens, GA, USA

e-mail: yiorgos@uga.edu

C. Campillo · S. Millán · M. d. H. Prieto

Centro de Investigaciones Científicas y Tecnológicas de Extremadura (CICYTEX), Finca La Orden, Junta de Extremadura. Guadajira, Badajoz, Spain

e-mail: carlos.campillo@juntaex.es

N. Graff

Agricultural Engineering Institute, Agricultural Research Organization, Volcani Institute, Rishon LeZion, Israel

The Robert H. Smith Faculty of Agriculture, Food and Environment, The Hebrew University of Jerusalem, Rehovot, Israel

Y. Saranga

The Robert H. Smith Faculty of Agriculture, Food and Environment, The Hebrew University of Jerusalem, Rehovot, Israel

J. Casadesús

Institut de Recerca i Tecnologia Agroalimentàries (IRTA), Centre UdL IRTA, Lleida, Catalonia, Spain

targets the spatial variability by using variable-rate irrigation (VRI) system or the temporal variability by using automatic triggering of the irrigation, (2) type of irrigation system, and (3) type of data the system uses for irrigation decisions. Each of the case studies addresses a unique combination of attributes and together they draw a more complement picture of precision irrigation. All case studies have shown that well-timed data provides decision support for VRI management, i.e. soil moisture sensor-data (south-eastern USA and Spain) and thermal aerial imagery (Israel). The three case studies showed that precision irrigation treatments performed better than uniform irrigation. Yield increased by 4.3–12% and water-use efficiency (WUE) was improved by 14–40%. The reliance on point-sensor data in the case studies from south-eastern USA and Spain dictated the use of pre-determined irrigation management zones (IMZ), yet, enabled adaptive in season irrigation management. In season remotely sensed images can be further used for adaptive IMZ, i.e. to modify their boundaries, yet it currently suits VRI in drip irrigation. From these case studies, it can be seen that full VRI implementation, which adapts for spatial and temporal changes, faces “site-specific” challenges, i.e. every irrigation system is unique, and thus requires tailored solutions.

Keywords Variable-rate-irrigation · Automatic-irrigation · Soil-sensors · Thermal-imagery · Decision support system

11.1 Introduction

Irrigation accounts for more than 70% of total water withdrawals on a global basis (The World Bank; <https://www.worldbank.org/en/topic/water-in-agriculture>). The inevitable competition between agriculture and other users of limited water resources will require that farmers become more efficient at producing crops with a finite water supply. In addition, because irrigated agriculture provides about 40% of the global food supply on 20% of the total cultivated land, the pressure to produce even more food on irrigated land will also intensify as global population increases. Productivity per unit of water consumed would increase by implementation of crop location strategies (optimal soil and climate attributes), conversion to crops with higher economic value, and adoption of alternate drought-tolerant crops as well as by the implementation of precision irrigation (Evans and Sadler 2008). These high-technology tools will not only allow adjustments of the water schedule depending on the needs of the crops at each moment and the characteristics of the soil, but will also increase the farmer’s expertise and be more attractive to new generations of young farmers. The term precision agriculture (PA) in general and precision irrigation in particular is perceived differently by stakeholders from research, extension, industry and by the farmers themselves. From the perspective of the research community, PA aims at improving productivity and sustainability by addressing spatial and temporal variation within fields. Automated irrigation scheduling is recognized as precision irrigation, and even though it does not address spatial variation, it addresses temporal variation. This chapter presents three case studies from south-eastern USA, Israel and Spain which relate to different attributes of precision irrigation: (1) type of

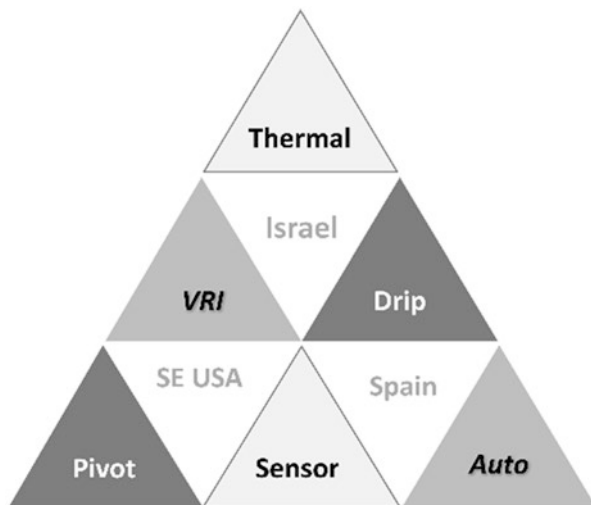


Fig. 11.1 Shared and complementary attributes of the case studies. White represents country; Outlined light grey represents type of input data; Dark grey represents the type of irrigation system and light grey (no outline) the type of precision irrigation

precision: whether it targets the spatial variation using a variable-rate irrigation (VRI) system or temporal variation by automatic triggering of the irrigation, (2) type of irrigation system and (3) type of data the system uses for irrigation decisions. Each of the case studies addresses unique combinations of attributes and together they draw a more complete picture of precision irrigation. Yet they are not totally separated from each other because they share some attributes which connect them (Fig. 11.1). The first case study from south-eastern USA describes VRI with centre pivots based on soil sensors, the second case study from Israel deals with variable-rate drip irrigation (VRDI) based mainly on thermal remote sensing, and the third case study from Spain presents an automatic drip irrigation system triggered by soil sensors. Figure 11.1 summarizes the shared and complementary attributes.

11.2 Case Study 11.1. Variable-Rate Irrigation with Centre Pivot in South-Eastern USA

11.2.1 Introduction

Precision irrigation has its roots in VRI technology developed for centre pivot irrigation systems by the University of Georgia (UGA) Precision Agriculture team in 2001 (Perry et al. 2002; Perry and Podcknee 2003). The UGA Precision Agriculture team recognized that variable-rate application of irrigation water was a key enabling technology for the adoption of PA in south-eastern USA. This was because fields in this region have very variable soil type and texture, moisture holding capacity and slope. If site-specific water needs are disregarded while attempting to vary other

inputs such as fertilizers, then this would not result in the desired gains in efficiency theoretically possible with PA. An additional reason was that in the south-eastern USA, irrigation of agronomic crops such as cotton (*Gossypium* spp.), maize (*Zea mays*), peanut (*Arachis hypogaea*) and soya bean (*Glycine max*), is now done almost exclusively with centre pivot irrigation systems.

Conventional centre pivots apply the same rate of water along the entire length of the pivot and cannot account for within-field variability or non-farmed areas. The UGA VRI technology was commercialized by FarmScan, an Australian electronics company. The large pivot manufacturers began offering their own VRI systems once the original patent expired in 2012.

The VRI allows centre pivots to vary water application rates along the length of the pivot using electronic controls to cycle sprinklers and control pivot speed. Sprinklers are controlled individually or together typically in groups of 2–10 depending on the level of resolution desired by the farmer. Each group or bank of sprinklers represents a grid with a 1–10-degree arc in which the application rate of irrigation water can be set as a percentage of the normal application rate; for example from 0 to 200% of normal (Fig. 11.2c). The number of degrees in the arc is determined by the level of resolution desired. A 50% application rate is half the normal rate and is achieved by cycling the sprinklers on and off every 30 s. A 150% application rate is achieved by leaving the sprinklers on continuously while decreasing the travel speed of the pivot. If other grids along the length of the pivot require smaller rates of application, the VRI controller adjusts the sprinkler cycling pattern within those grids accordingly.

The VRI can be installed retroactively on most existing pivots. Installation costs vary widely by brand and are also a function of the length of the pivot and the level of resolution desired by the farmer to address the variability of the field. Application rates are determined from an application or prescription map. A short video describing VRI is available at (https://www.youtube.com/watch?v=DgexX_IToI0).

11.2.2 Prescription Maps

The prescription map for a field is developed jointly by the farmer and VRI dealer on desktop software (Fig. 11.2a, b, c) and then downloaded to the VRI controller on the pivot. The field is divided into irrigation management zones (IMZs) and application rates assigned to each of the IMZs using whatever information is available. In almost all VRI applications, the prescription maps are static. In other words, they are typically developed once and used thereafter. Static prescription maps do not respond to environmental variables such as weather patterns and other factors that affect soil moisture conditions and rates of crop growth. Although VRI offers a great leap forward in improving water-use efficiency (WUE), the system can be greatly enhanced with real-time information on crop water needs to control the application rates. One approach for creating dynamic prescription maps is to use soil moisture sensors to estimate the amount of irrigation water needed to return each IMZ to an

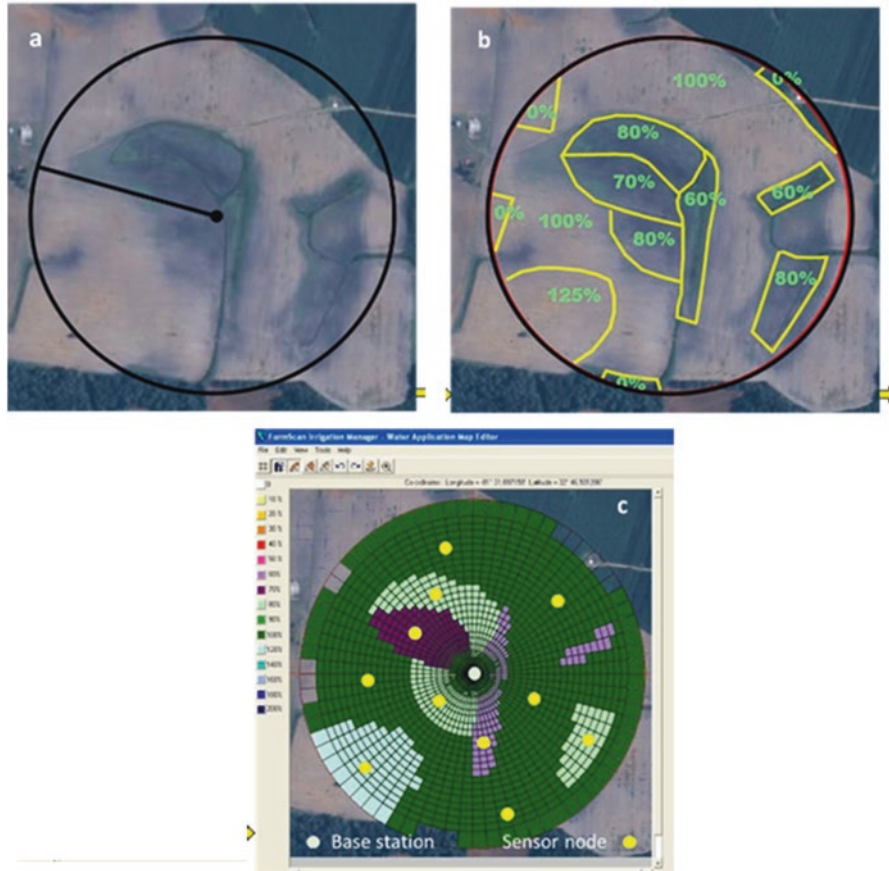


Fig. 11.2 The process of creating a VRI prescription map for a 49-ha field in Georgia. A bare-soil image is used as a base map to delineate IMZs (a). The percentages in (b) indicate the percent of the normal application rate assigned to each IMZ. Grid cells in (c) represent discreet areas that can receive unique application rates. Cells grouped into the same colour represent the IMZs delineated in (b). The yellow circles represent potential locations of soil moisture sensor nodes

ideal soil moisture condition (Fig. 11.2c). This case study describes the on-farm application of a *dynamic* VRI control system developed by the UGA Precision Agriculture Team. The control system couples real-time soil moisture sensing networks, an irrigation scheduling decision support system (DSS), and VRI.

11.2.3 A Dynamic VRI System

The operational paradigm of the UGA dynamic VRI control system is that the field is divided into IMZs and a soil moisture sensing network with a high density of sensor nodes is installed to monitor soil conditions within the IMZs. Between one and

three nodes are installed in each IMZ depending on the zone’s size. Soil moisture data are uploaded hourly to a web-based user interface.

At the web-based user interface, the soil moisture data are used by the DSS running in the background to develop irrigation scheduling recommendations for each IMZ. The recommendations are then approved by the user (farmer) and downloaded wirelessly to the VRI controller on the pivot as a precision irrigation prescription. When the pivot is engaged by the farmer, the pivot applies the recommended rates. Figure 11.3 shows the dashboard of the UGA dynamic VRI system.

11.2.3.1 Real-Time Soil Moisture Sensing Network

A key requirement of a soil moisture sensor based dynamic VRI system is a dense network of sensor nodes that is inexpensive, reliable, wireless, energy efficient, easy to install and remove, and that does not interfere with farming operations. These types of networks are only now becoming commercially available. The UGA smart sensor array (UGA SSA) soil moisture sensor network was specifically developed for the dynamic VRI system described here.

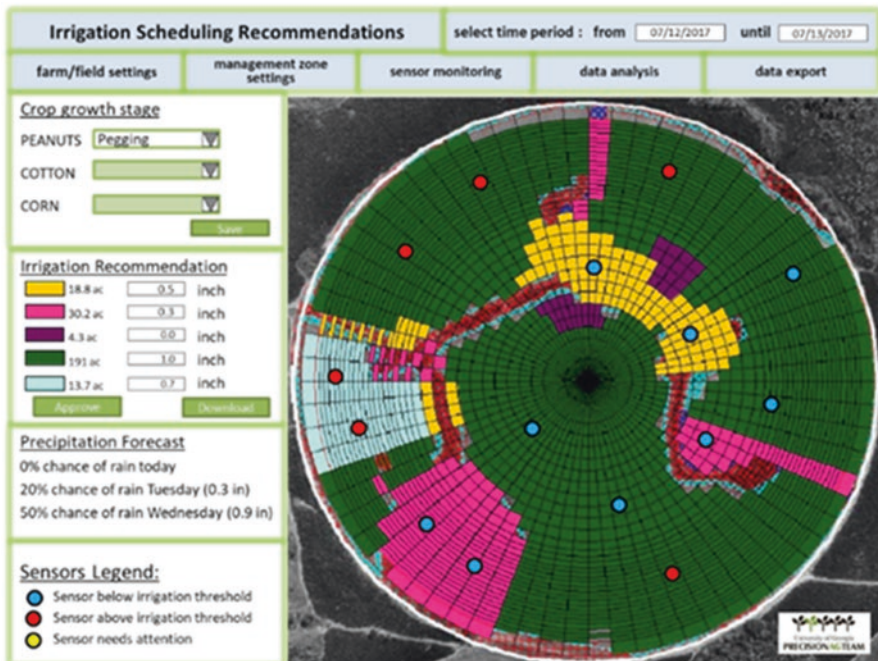


Fig. 11.3 Dashboard of the UGA dynamic VRI system as seen by the user. The system requires the user to approve and then download the daily prescription map to the VRI controller located on the pivot. Real-Time Soil Moisture Sensing Network

The UGA SSA consists of smart sensor nodes and a base station. The term sensor node refers to the combination of electronics and sensor probes installed within a field at a single location. The electronics include a circuit board for data acquisition and processing, and a radio frequency (RF) transmitter. The UGA SSA uses Watermark® soil moisture sensors that measure soil moisture in terms of soil water tension (SWT)—the absolute value of soil matric potential in units of kilopascals (kPa). Each soil moisture probe integrates up to three Watermark® sensors. In addition, each node supports two thermocouples for measuring soil and or canopy temperature. For deep-rooted field crops like cotton or maize, the sensors on the probe are arranged so that when installed they are at 20, 40 and 60 cm below the soil surface although any combination of depths is possible. For shallow-rooted crops like peanut, 10, 20 and 40-cm depths are used. Users access the data through a dedicated web-based user interface.

11.2.3.2 Web-Based User Interface and Decision Support System

The purpose of the web-based interface is to allow users to visualize their soil moisture data and to make irrigation recommendations for each IMZ. A PHP (Personal Home Page) and JavaScript programming languages were used to create different visualizations of the soil moisture data (Fig. 11.4). The different visualizations provide users with the opportunity to view instantaneous SWT, time series of SWT and IMZ delineation of their fields. The user interface was smartphone compliant.

The web-based user interface also included a DSS which offers irrigation recommendations for each IMZ (Liakos et al. 2015). The DSS uses a modified Van Genuchten model to convert SWT data to volumetric water content (Liang et al. 2016). The strength of the method is that it uses soil properties readily available from the United States Department of Agriculture – Natural Resources Conservation Service (USDA-NRCS) Web Soil Survey (<https://websoilsurvey.sc.egov.usda.gov/>) to translate measured SWT into irrigation recommendations that are specific to the soil moisture status of each IMZ. The DSS uses mean SWT data collected at 07:00 h from all nodes within an IMZ to calculate the volume of irrigation water needed to bring the soil profile back to the desired soil moisture condition, which could be field capacity or a percentage of field capacity (for example 75% of field capacity) (Fig. 11.5). Each node's SWT value is a weighted average of the SWT values of the three Watermark® sensors of the node as shown in Eq. (11.1) where α , β and γ are weighting factors based on the phenological stage of the crop. Early in the growing season when the root system is not fully developed, more weight is given to the shallow sensors. As the root system develops, the weighting factors change accordingly. For peanut, at maturity, α , β and γ were 0.5, 0.3 and 0.2 respectively. Weighting factors may differ by crop.

$$\text{Weighted SWT} = \alpha \times \text{SWT}_{10\text{cm}} + \beta \times \text{SWT}_{20\text{cm}} + \gamma \times \text{SWT}_{40\text{cm}} \quad (11.1)$$

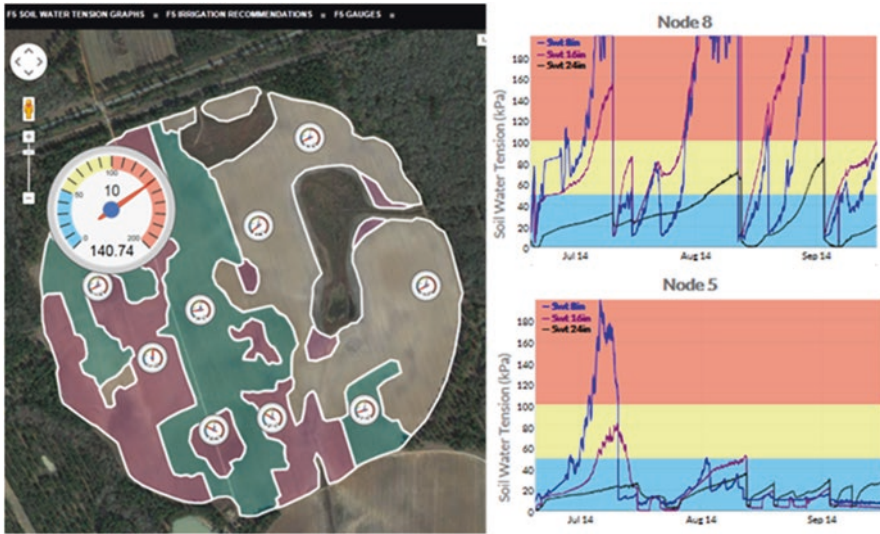


Fig. 11.4 Two different visualizations of UGA SSA data. On the left is current SWT displayed through colour coded gauges. Touching the gauges with the cursor or finger enlarges them. On the right are SWT curves for three depths for the entire growing season. Note the difference in response between nodes in the same field

Irrigation recommendations may use the same SWT threshold across all of the crop's phenological stages or thresholds could be adjusted by phenological stage. For example, UGA cotton physiologists recommend a 70-kPa threshold before flowering and a 40-kPa threshold after flowering (Meeks et al. 2017).

11.2.3.3 On-Farm Testing of the UGA Dynamic VRI Control System

The UGA dynamic VRI control system was field-tested on commercial farms with funding from the United States National Peanut Board's Southern Peanut Research Initiative (SPRI). Because of the funding source, the work was conducted with peanut (*Arachis hypogaea* L.). A farmer who already operated several VRI-enabled centre pivots was recruited to participate in the project. Before this project, the farmer had used his VRI systems only to turn sprinklers off over non-farmed areas in the field. He had not varied application rates over farmed areas. The evaluation compared the performance of the dynamic VRI control system to the farmer's standard method for scheduling irrigation on large fields. The case study below describes the on-farm evaluation conducted in 2017.

The 94-ha field was divided into IMZs using soil electrical conductivity, digital elevation models (DEMs), hydrography and the Management Zone Analyst geostatistical software (MZA) (Fridgen et al. 2004). Eight alternating 120-row wide (109 m) conventional irrigation and precision irrigation strips were then



Fig. 11.5 The experimental design of the field used in the 2017 case study showing four pairs of parallel VRI and conventional strips (brown). The VRI strips maintain the delineated IMZ. The yellow circles indicate the location of 30 UGA SSA sensor nodes. The table to the right indicates the depth of water that is recommended for each IMZ by the DSS. The recommendations are provided for shallow and deep-rooted crops

superimposed over the IMZs. The precision irrigation strips retained the IMZ boundaries while the conventional strips did not (Fig. 11.5). After planting, UGA SSA sensor nodes were installed in each of the IMZs in the precision irrigation strips. Sensor nodes were located close to the centre of each IMZ to avoid boundary effects created by changing the rates of water application as the VRI system transitioned from one IMZ to another. Three sensor nodes were also installed in each of the conventional strips. A total of 30 nodes, 22 in IMZs and 8 in the conventional strips, were installed. Each probe contained Watermark® sensors at 10, 20 and 40-cm depths below the soil surface.

The UGA SSA sensor probes installed in the conventional irrigation strips were used only to monitor soil moisture conditions. Each conventional strip was irrigated uniformly by the farmer using Irrigator Pro (Davidson Jr. et al. 2000) to make irrigation decisions. Irrigator Pro is a public domain peanut crop growth model and irrigation scheduling tool developed by USDA that uses soil temperature, ambient temperature and precipitation to provide yes/no irrigation decisions for peanuts. The user decides how much water to apply. The farmer installed his own soil thermometers and a rain gauge in the field and manually collected data two to three times a week. He then entered the data into the Irrigator Pro model running on his personal computer to make irrigation decisions. Each uniform strip was irrigated uniformly.

All irrigation decisions and the amount of irrigation water applied for the precision irrigation strip IMZs were made using the DSS. At each irrigation event, the DSS used mean weighted SWT from each IMZ to calculate the irrigation water

needed to return the soil profile of the zone to 75% of field capacity. The irrigation recommendations for each IMZ were then transferred manually to the prescription map that was downloaded wirelessly to the pivot VRI controller. In this field, approximately 72 h were required for the pivot to irrigate the field. Because of this, a new prescription map was downloaded every morning during an irrigation event to address soil moisture changes that occurred over the past 24 h.

11.2.3.4 Yield and Water-Use Efficiency

Yield was aggregated by strip. Water-use efficiency (WUE) was calculated by dividing yield by the irrigation applied to each strip. The 2017 peanut growing season was relatively dry with 272 mm of precipitation, which is about half of the normal precipitation received in this area. Since each IMZ within the VRI strips received different amounts of irrigation, the irrigation assigned to each VRI strip was weighted by the area of each IMZ. Table 11.1 presents a summary of the results. Every VRI strip had greater WUE than the conventional uniformly irrigated strips. Three of the VRI strips had larger yields than the uniform strips. Overall, the VRI strips resulted in a 39.7% increase in WUE and 4.3% more yield.

11.2.4 Conclusions

Pivot manufacturers have observed the outcomes of this study and dynamic VRI experiments conducted by other research groups and have begun to develop their own solutions to this issue. Lindsay Corporation which manufactures the Zimatic brand centre pivot irrigation systems is offering its version of dynamic VRI under the trade name of FieldNET® Advisor (<https://www.lindsay.com/usca/en/irrigation/brands/fieldnet/resources/>). This system uses FAO-56 type evapotranspiration models to estimate daily crop water use in each IMZ. This estimate and soil properties from the NRCS Web Soil Survey are used to calculate a daily soil water balance. When the soil water balance reaches a predetermined threshold, the IMZ is irrigated. Data from the model automatically populate a prescription map that is downloaded wirelessly to the pivot's panel. This is likely to be a more adoptable dynamic VRI solution until sensor costs are greatly reduced and installation and removal requires less effort than current sensor solutions. However, models might not

Table 11.1 Comparison of results between the VRI and Uniform treatments for the entire field

Treatment	Area (ha)	Yield (kg ha ⁻¹)	Avg Irrig (mm)	WUE (kg ha ⁻¹ mm ⁻¹)	% Diff Yield	% Diff WUE
VRI	22.5	5983	91	66	4.3	39.7
Uniform	24.2	5735	122	47		
Totals	47					

account accurately for soil differences within IMZs that may be accounted for with a high-density sensor network.

11.3 Case Study 11.2. Variable-Rate irrigation with Drip irrigation in Israel

11.3.1 Introduction

Approximately half of the agricultural land in Israel is irrigated and the majority of that (around 60%) is irrigated with drip systems. The widespread implementation of drip irrigation has made a major contribution to the increase in irrigation water-use efficiency (WUE) in Israel, in terms of production per irrigation unit. Irrigation WUE in Israel has increased steadily since the 1960s and doubled in the period 2000–2010. Yet, it hardly changed after 2011. Evans and Sadler (2008) argue that emerging computerized GNSS-based precision irrigation technologies for self-propelled sprinklers and micro-irrigation systems will enable growers to apply water and agrochemicals more precisely and site-specifically to match soil and plant status and needs using wireless sensor networks. While VRI technology for centre pivot irrigation systems goes back to the 2000s and is already implemented by farmers (case study 1 from south-eastern USA), it is still under development for micro irrigation systems like sprinklers and drip systems.

There are two primary challenges for variable-rate drip irrigation (VRDI) development: a lack of mobility and a lack of variable-rate emitters. A few recent studies have applied VRDI in vineyards (e.g. McClymont et al. 2012; Nadav and Schweitzer 2017). To overcome the lack of mobility, the vineyards were subdivided into management zones each with valves and piping necessary for autonomous irrigation. The abovementioned studies differed in zonation methodology. McClymont et al. (2012) assumed relative stability of the IMZ condition over time, i.e. a zone with less vigour in 1 year was assumed likely to exhibit less vigour in other years. Accordingly, the vineyard was designed to irrigate a few pre-determined management zones that differed in size and shape based on multi-year NDVI maps and a canopy temperature map. In this way, the number of valves and hence the cost of the system is reduced. In contrast to this, several studies have shown that IMZs are dynamic and can change from year to year and vary even during a single season (O'Shaughnessy et al. 2015; Scudiero et al. 2018). Sanchez et al. (2017) and Bahat et al. (2019) used a 'blind' zonation based on regular polygons of equal sizes allowing greater flexibility and adaptation to in-season spatial changes of IMZ. Despite differences in zonation approach, and how irrigation decisions were made for each zone, all have shown a decrease in spatial variation in yield or in water status. Currently, there are no off-the-shelf VRDI systems, but prototypes have already been installed and tested in a few orchards.

This section described how precision irrigation studies in Israel have evolved over the last 20 years following three central themes, i.e. (1) thermal imaging collection and analysis to map the variation in water status, (2) creation of irrigation prescription maps and (3) implementing variable-rate drip irrigation to address variability in a commercial field.

11.3.2 Thermal Imaging for Mapping Variation in Water Status

Drip irrigation is very efficient compared to other irrigation systems, therefore, most of the precision drip irrigation studies in Israel have focused on crops that it would benefit most: cotton and vineyards. Both cotton and wine grape (*Vitis vinifera*) vineyards are grown under controlled regimes of water stress, therefore, the best irrigation practices involve monitoring of plant water status. This section focuses on cotton. In Israel, irrigation scheduling is predetermined and water stress corrections are made by modifying irrigation amounts.

Quantities of irrigation water are estimated according to the equation:

$$\text{Irrigation quantity} = \alpha \times K_c \times ET_0 \quad (11.2)$$

where ET_0 is the reference evapotranspiration, (K_c) is the crop coefficient (FAO56; Allen et al. 1998) and α is the water status (or water stress) coefficient. Real-time daily values of ET_0 for many locations in Israel are available from the Ministry of Agriculture and Rural Development's (MARD) Agro-meteorology website (meteo.co.il). The K_c tables are also available on the web, For example, this is the link for cotton: https://www.moag.gov.il/shaham/professionalinformation/documents/daily_exhalation_user_guide_2014.pdf. In addition, an app was developed for most crops by MARD's Extension Service (<https://play.google.com/store/apps/details?id=il.gov.moag.shaham.irrigationapp>). The K_c of cotton while in its vegetative growth stage is further adjusted according to the rate of plant growth and in the boll-filling period to a measure of plant water status, leaf water potential (LWP). For these, growers measure, among other properties, height and LWP of a few plants in the field once or twice a week. Based on target curves of these properties that were developed by the cotton board they can estimate crop water status, α , and further correct irrigation quantities. Direct plant measures are reasonably reliable and reflect individual plant water status, but they do not represent the spatial variability of water status in the plot and are laborious and therefore expensive.

Thermal infrared (TIR) images have been used in most of the precision irrigation studies as alternatives for estimating and mapping water status in the productive periods. Initial studies focused on correlating the crop water stress index (CWSI) (Idso et al. 1981) extracted from thermal images and leaf or stem water potential (Cohen et al. 2005; Möller et al. 2007). The CWSI is defined as follows:

$$\text{CWSI} = \frac{T_{\text{canopy}} - T_{\text{wet}}}{T_{\text{dry}} - T_{\text{wet}}} \quad (11.3)$$

where T_{canopy} is leaf or canopy temperature, and T_{wet} and T_{dry} are approximations of minimum and maximum canopy temperatures, respectively. Correlations between CWSI calculated using ground-based thermal images and LWP/SWP in both cotton and vines were strong ($r = 0.85\text{--}0.92$). Further studies examined whether robust relationships exist between the two measures throughout a cotton growing season, for different varieties, across years and in different geographical areas (different climates and soils) (Cohen et al. 2015). To test this, a dataset from three cotton growing seasons and from different geographical areas was created. A linear CWSI–LWP relationship was found to be appropriate, and had with a high coefficient of determination ($r = 0.84$).

To upscale the use of thermal imaging to commercial application, aerial thermal images over commercial cotton fields were used to map the variation in LWP and to produce prescription maps according to water status levels (Cohen et al. 2017b). Transformation of raw aerial thermal images into CWSI to be used further to map LWP requires a simple, rapid and yet accurate procedure to extract T_{wet} . An extensive comparison between various wet baselines that were used to calculate CWSI in cotton have shown the superiority of bio-indicator wet baselines including the average temperature of the coolest 5–10% of the canopy pixels in the overall field (Alchanatis et al. 2010; Rud et al. 2014; Gonzalez-Dugo et al. 2013). Furthermore, the statistical bio-indicator for wet-baseline (T_{wet}) has minimal requirements (measurements of air temperature) compared to other existing alternatives, thus paving the way towards commercialization.

Based on bio-indicators, prescription-like maps which were based on the LWP recommended curve for several commercial fields were produced on three dates during the season (Fig. 11.6 presents maps for one of the fields). The variation in water status was not constant (Cohen et al. 2017b). The maps show the importance of in-season mapping of the variation for rational irrigation management. This means that to improve VRI, in-season IMZ's should be used.

11.3.3 Thermal-Based Water Status Maps for Irrigation Management

11.3.3.1 Irrigation Management Experiment in Cotton

Cotton is an important crop in the crop rotation widely practiced in Israel. Cotton yield and quality are very dependent on an adequate supply of water and in the boll-filling growth stage they are grown under controlled water stress to allow balance between vegetative growth and cotton production. While it has been proved efficient,

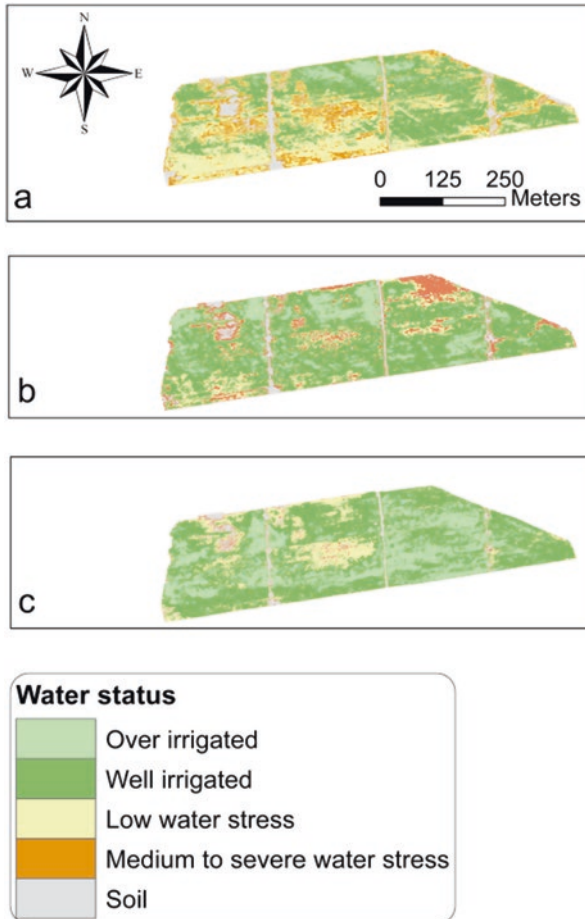


Fig. 11.6 Multi-temporal LWP variability maps of a 15 ha commercial cotton fields in Yavne, Israel. The LWP maps are based on aerial thermal images acquired on 10/7/11 (a), 27/7/11 (b), 18/8/11 (c)

adoption of LWP as a complementary tool for irrigation management has been limited because of the time and manpower needed to obtain manual measurements. In addition, these measurements do not necessarily represent the entire field or its variability. The experiment described in this section compared thermal-imaging based irrigation management to LWP-based management (Rosenberg et al. 2014).

Field Plots and Irrigation Treatments:

Field measurements were conducted in the summer of 2013 at Kibbutz Givat Brener, Israel. Experimental plots were planted with cotton, *Gossypium hirsutum* × *Gossypium barbadense* hybrid (“Acalpi”) at the beginning of April and were drip-irrigated with one drip line every other row. Each plot was 18 m × 19 m. Plots

were irrigated with four different treatments and with six replicates (a total of 24 sub-plots). Irrigation amounts were determined based on ET_0 and crop coefficients, and stress factor (α) corrections were made according to height measurements in the vegetative period and LWP in the boll-filling period. The treatments differed by the estimation stress factor α and thus the irrigation amounts. In one treatment, denoted Reg-LWP, α was estimated according to the commercial practice, i.e. based on a few direct LWP measurements conducted twice a week and irrigation decisions were made based on a recommended LWP curve. In the three other treatments, denoted Reg-TIR, Def-TIR (deficit irrigation) and Oir-TIR (over-irrigation) α was estimated based on LWP calculated by thermal images acquired once a week. Different LWP curves were used for the different treatments. In Reg-TIR, like the Reg-LWP, irrigation decisions were based on a recommended LWP curve. In Def-TIR and Oir-TIR, irrigation decisions were based on water saving and over-irrigation LWP curves, respectively.

Image Acquisition:

Oblique thermal images were acquired above the experimental plots using uncooled infrared thermal cameras (SC655 and SC2000, FLIR systems, Oregon, USA) that were attached to a vertical 20 m mast (mounted to a tractor). The two cameras are sensitive in the thermal range of 7.5–13 μm and have measurement sensitivity and accuracy of 0.1 $^{\circ}\text{C}$ and ± 2 $^{\circ}\text{C}$, respectively. Image acquisition was carried out on 4 days in the boll-filling period: 04/08/13, 11/08/13, 18/08/13 and 25/08/13. The thermal images were acquired a few hours before irrigation, around solar noon (11:00–15:00 h daylight saving Israel Standard Time, GMT +3).

Processing of Thermal Images and LWP Calculation:

To estimate T_{canopy} separation between vegetation and background pixels in the thermal images was first done empirically following Meron et al. (2010). Second, the mean canopy temperature was extracted for each sub-plot. The CWSI was calculated according to Eq. (11.3). The T_{dry} was used in its empirical form, i.e. $T_{\text{air}} + 5$ $^{\circ}\text{C}$ which gave a reasonable estimate of the maximum leaf temperature for cotton (Alchanatis et al. 2010). To estimate T_{wet} temperature, a reference strip adjacent to the experimental plot was double irrigated using a drip-line every row. The temperature of this strip was extracted each time from the thermal images similar to the extraction of the T_{canopy} . Last, LWP was determined from a linear CWSI–LWP relationship (Eq. 11.4) based on a multi-year database (Cohen et al. 2015).

$$\text{LWP} = -1.77\text{CWSI} - 1.28 - K \quad (11.4)$$

where K is a transformation constant between the LWP [MPa] measurement methodology and other methodologies (Cohen et al. 2017b).

The LWP Measurements:

Parallel to image acquisition, 4–6 leaves from each replicate were sampled and their LWP was measured with a pressure chamber (model ARIMAD 1, Mevo Hama Instruments, Israel), as described by Meron et al. (1987).

11.3.4 Results

The CWSI-based and measured LWP were well correlated with $r = 0.88$ and RMSE of 0.14 MPa. In addition, the slope of the regression model was not significantly different from 1.

Until day 30 from onset (21/07/2013) the entire field received homogeneous irrigation of 316.4 mm. From 31 days after onset, treatments were irrigated differently as LWP measurements or calculations were used for K_c corrections. From 22/7/2013 until 28/8/2013 Def-TIR and Oir-TIR received 70.6 and 156.1 mm, respectively while Reg-LWP and Reg-TIR received very similar irrigation amounts (96.5 and 90.0 mm, respectively). Figure 11.7 shows the yield and irrigation water-use efficiency (WUE) of the four treatments. The WUE here was not calculated for the seasonal irrigation amounts but for the irrigation amounts given during the irrigation experiment (during the reproductive stage; from 31 days after onset onwards). The yields of the different treatments were very similar (*one-way ANOVA*, $F = 0.26$, $p = 0.85$). In terms of irrigation amounts, both regular treatments (Reg-LWP and Reg-TIR) were larger than the deficit irrigation treatment and smaller than the over-irrigation treatment. Significant differences were found in WUE (*one-way ANOVA*, $F = 169.9$, $p < 0.01$; $n = 24$). With a standard error of the difference (SED) of 1.3 and least significance difference (LSD) of 2.7 it can be said that WUE of Reg-TIR ($88.3 \text{ kg mm}^{-1} \text{ ha}^{-1}$) was significantly larger than that of Reg-LWP ($79.1 \text{ kg mm}^{-1} \text{ ha}^{-1}$) (Fig. 11.7). The results suggest that remotely sensed thermal data can replace direct pressure chamber measurements, while maintaining at least the same yield with similar amounts of water application. Furthermore, it has the potential to improve WUE. It is assumed that despite the imperfect estimation of LWP measurements by the thermal images, the images can represent most if not all the plants leading to sound irrigation decisions.

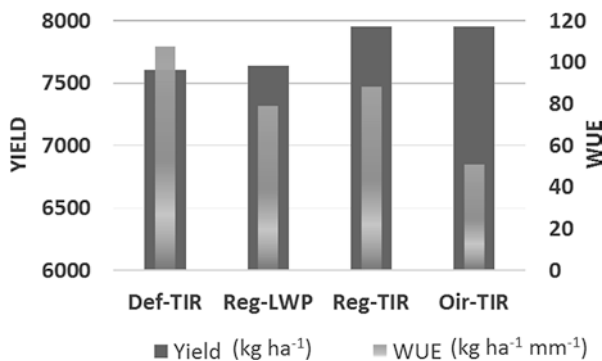


Fig. 11.7 Yield and irrigation water-use efficiency (WUE) for every irrigation treatment. The WUE was calculated from the irrigation given at the reproductive stage only

11.3.4.1 Addressing the Natural Variation in Water Status in a Commercial Cotton Field

The experiment in Givat Brener, described above, demonstrated the ability of thermal based LWP maps to aid irrigation decisions by correcting K_c . As mentioned above, variable-rate drip irrigation is challenging and its efficiency should be justified by either increasing yield and or WUE and or reducing variability. For that, an experiment was conducted in a highly variable zone in a commercial cotton field in Bnei-Darom farm near to the coastline plain of southern Israel, a well-known area for cotton cultivation. This experiment aimed at demonstrating the implementation of VRI in a drip irrigation system and its efficiency compared to unified commercial irrigation. The northern part of the field is characterized by considerable natural variability in soil type and water holding capacity. Figure 11.8 shows there is a patch of sandy soil in the northern part of the field (white arrow). The experimental area was divided into three treatments, one commercial and two VRIs, denoted COM, VRI, TIR (Fig. 11.8a) with 8 blocks (Fig. 11.8b) assuming each block to have similar soil texture characteristic. Every treatment was divided into eight cells (24 m wide by 30–40 m long), giving a total of 24 cells. From each, a soil sample was taken for texture. In addition, the height of three plants was measured twice a week in every cell from May to July, and LWP of four leaves was measured once a week from July to the end of August (boll-filling period). All treatments were irrigated similarly by the farmer until the boll-filling period (beginning of July). In general, the farmer followed the cotton board recommendations, but he added 10% to the recommended irrigation amounts relying on his experience that this area is sandy and requires more water. From the boll-filling period, the commercial treatment (COM) was irrigated by the farmer as for the Reg-LWP described in the previous section. The VRI and TIR were irrigated as for Reg-TIR, i.e. LWP was calculated from CWSI extracted from weekly aerial thermal images. The two treatments were differentiated by the size of their management cell (Fig. 11.8a). In TIR, the eight cells were grouped into two irrigation units (outlined in green in Fig. 11.8a), i.e. the northern and southern four cells were irrigated individually based on their averaged calculated LWP. In general, the northern cells are sandier (62% on average) than the southern cells (41% on average). In VRI, each of the eight cells (outlined in black in Fig. 11.8a) were irrigated individually based on their averaged calculated LWP. Figure 11.8a presents the map of accumulated irrigation amounts for each irrigation unit. Focusing on both VRI treatments (VRI and TIR), it can be seen that the northern areas were irrigated more than the southern areas, which are less sandy and experienced less water stress (as indicated by their calculated LWP in different dates, data not shown).

The unified irrigated strip (COM) was irrigated with 476 mm and 386 mm in the northern and southern irrigation units, respectively. The northern and the southern irrigation units of TIR treatment were irrigated with 440 mm (−8% vs COM) and 347 mm (−10% vs COM), respectively. Irrigation in the VRI strip ranged between 329 mm (−15% vs COM) and 590 mm (+24% vs COM). Table 11.2 presents a summary of the yield (before ginning) and WUE results. Yield for the whole

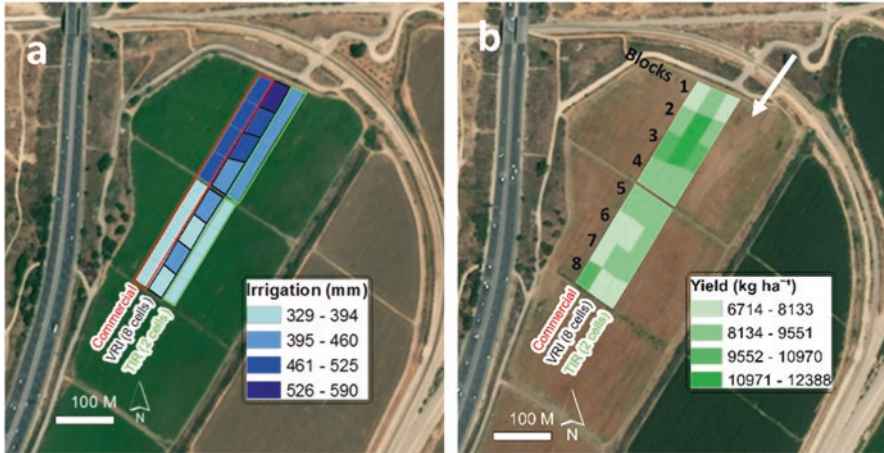


Fig. 11.8 Treatment borders and accumulated seasonal irrigation (a) and yield (b) for every cell. The white arrow marks a patch of sandy soil

experiment area ranged between 6714 and 12 388 kg ha⁻¹ and WUE ranged between 15.7 kg ha⁻¹ mm⁻¹ and 26.6 kg ha⁻¹ mm⁻¹. No significant differences were found between blocks in both yield and WUE and no significant differences were found between treatments (*Two-way ANOVA, no repetition, p > 0.05*). Four of the VRI blocks had larger yields than uniform irrigation (COM) while three blocks had smaller yields. Additionally, in four of the VRI blocks greater WUE was observed compared to the conventional uniformly irrigation (COM). Overall, the VRI treatments resulted in 6% more yield and 4% increase in WUE. The TIR treatment showed lower performance in yield (-3.2%) while better performance in WUE (6.1%). It might be related to the precision scale. The TIR treatment represents a lower resolution of VRI having only two irrigation units compared with eight irrigation units of the VRI. A similar experiment was conducted in the 2019 season in which VRI was practiced throughout the whole irrigation period. In the 2019 experiment seven out of eight blocks had more yield and WUE than the uniform irrigation treatment (COM). The VRI treatments resulted in 15.5% more yield (not significant) with 17.4% larger WUE (significant; data not shown).

11.3.5 Conclusions

Multi-year studies on thermal-remote sensing for water status mapping and for irrigation management have been summarized briefly. The results suggest that remotely sensed thermal data can replace manual measurements of water status, with the same or higher yields and similar or less amounts of water application. Thus, thermal imaging has the potential to improve WUE. It is assumed that despite the imperfection in the estimation of LWP by thermal imaging, the latter has the advantage of

Table 11.2 Comparison of results between the VRI, TIR and Uniform (COM) treatments by blocks

	Block	Com	TIR	VRI	% Diff TIR	% Diff VRI
Yield (kg ha ⁻¹)	1	7997	7609	9282	-5	16
	2	9263	9392	12388	1	34
	3	10398	10467	12108	1	16
	4	9103	8765	9199	-4	1
	5	9531	8674	8718	-9	-9
	6	7794	8674	7276	11	-7
	7	7013	9104	9444	30	35
	8	10593	6714	7519	-37	-29
	Avg.	8961	8675	9492	-1.4	7.2
WUE (kg ha ⁻¹ mm ⁻¹)	1	18.68	17.30	15.73	3	-6
	2	21.64	21.35	26.65	10	37
	3	24.29	23.79	25.19	9	15
	4	22.27	19.92	20.58	4	8
	5	22.27	21.85	22.09	1	-10
	6	18.21	21.85	19.28	24	-4
	7	16.38	22.93	21.99	44	21
	8	24.75	16.91	22.87	-30	-17
	Avg.	20.94	20.74	20.55	1.2	4.0

measuring many more of the plants, leading to better irrigation decisions. Another step towards the implementation of this technique was a field irrigation experiment in which natural variation of water status in a commercial cotton field was addressed by variable-rate drip irrigation. Larger, though not significant, yields were obtained. Since this is the first attempt in using VRDI in field crops, more experiments should be conducted to prove its added value. Thermal imaging, however, can be used not only for VRI but also for better estimation of the field water status and to improve irrigation decisions. Because of its relatively high cost, to assimilate thermal imaging for commercial use more cost effective methods should be developed (Cohen et al. 2017a).

11.4 Case Study 11.3. Automatic Irrigation of Orchards Using Soil Moisture Sensors (IRRIX Model)

11.4.1 Introduction

At the scientific level, the processes that determine the water demand of crops are well known, and various methodologies have been developed to improve irrigation efficiency. The water balance method, in which the water inputs of the soil-plant system must be balanced to the expected outputs (Allen et al. 1998), is the most

widely used system to determine the irrigation needs of a crop. One of the drawbacks of the water balance method is that any inaccurate parameterization will produce a systematic error that will accumulate throughout the crop cycle due to deviations that occur between estimated values and actual consumption. Irrigation control based on feedback from moisture sensors is a viable alternative to the water balance method, having as its main advantage the ability to adjust irrigation to the needs of a specific plot (Casadesús et al. 2012). However, there are also drawbacks to irrigation control based only on sensors such as the risk of sensor breakdown, variability in the measurements (Nolz and Kammerer 2017) and difficulty in interpreting sensor results, especially for drip irrigation where soil water distribution is heterogeneous.

In general terms, as both the water balance and sensor-based irrigation control methods have their pros and cons, combining both approaches seem to be the best way to improve the efficiency of irrigation in agricultural systems. This can be done by determining the irrigation dose from a water balance model and then using sensors to adjust that model to the real situation of each plot. Information and communication technologies (ICTs) can be used to attain this objective. In the last decade, most of the studies that have been published on automatic irrigation controllers have focused on regulating soil water content (SWC) or soil water tension (SWT) with feedback-based on/off strategies (Luthra et al. 1997; Miranda et al. 2005; Cáceres et al. 2007; Tahar et al. 2011). These devices are relatively inexpensive and easy to use, but ground water measurements imply certain limitations: they require a large number of sensors and do not consider plant status and response. Xiang (2011) and Zhu and Li (2011) published a study on irrigation controllers that used a combination of SWC and weather data to control drip irrigation. Romero et al. (2012) concluded that the approach of combining weather data with soil moisture signals could increase irrigation efficiency in almond trees. O'Shaughnessy and Evett (2010) and Peters and Evett (2008) proposed irrigation controllers aimed at regulating canopy temperature instead of SWC sensors.

Software tools and web applications are of fundamental importance when it comes to determining when and how much irrigation should be applied in response to crop development, crop type and environmental conditions (Casadesús et al. 2012). Various computer software packages have been developed to monitor soil properties and irrigation scheduling over a wide range of irrigation systems (Hess 1996; Abreu and Pereira 2002). Kim and Evans (2009) developed decision support software to collect information from wireless sensor networks (WSN) and control a site-specific linear-move irrigation system on a malting barley (*Hordeum vulgare* L.) field. A similar approach was described in the first case study of this chapter. There are also researchers who have developed software tools that allow operation in combination with the water balance approach and crop evapotranspiration (ET_c) estimation using soil or plant humidity sensors to enable subsequent readjustment of the ET_c estimation (Bacci et al. 2008; Casadesús et al. 2012; Osroosh et al. 2016). In addition, there are researchers who used a DSS that executed a pre-established irrigation schedule in which regulated deficit irrigation (RDI) was applied without human intervention in a Japanese plum crop (*Prunus salicina*) (Millán et al. 2019).

and a hedgerow olive orchard (Millán et al. 2020) combining the water balance method with soil moisture sensors.

11.4.2 *Semi Commercial Testing of an Automatic Irrigation System*

To demonstrate the use of an automatic irrigation system (IRRIX), an experiment was conducted during 2018 (FERTINNOWA Project) on a commercial farm called “Finca El Chaparrito”. The farm belongs to the company Haciendas Bio S.A., and is in the municipality of Pueblonuevo del Guadiana, Badajoz (latitude 38°5 6′ 13.59″ N, longitude 6° 45′ 21.98″ W, WGS84), Spain. Three different varieties of early-maturing peach (*Prunus persica*) were present in the measurement area (4.5 ha): Kay-sweet (1.5 ha), Almaneb (1.5 ha) and UFO-4 (1.5 ha). All trees were planted in the spring of 2009 at a spacing of 5 m × 3 m, in an east-west row orientation. The trees were irrigated daily using a drip system with a single lateral line per tree row located 0.5 m from the base of the tree and on-line emitters with discharge rates of 2.2 l h⁻¹, spaced at 0.5 m. The irrigation sector was separated into two parts for each variety, thus allowing the establishment of two irrigation management systems for each variety.

11.4.2.1 Selection of the Testing Zone

An analysis of soil and plant spatial variation was carried out to select the best area to install the IRRIX system and enable comparison between it and the irrigation system carried out by the farmer (FARMER). For this purpose, the most homogeneous zone possible was selected. To determine soil heterogeneity, the apparent electrical conductivity (EC_a) of the soil was measured with a Dualem-1S non-contact sensor (Dualem, Inc., Milton, Ontario, Canada), equipped with a global positioning system (GPS) antenna. The entire field was surveyed for EC_a, obtaining both shallow (0–50 cm) electrical conductivity (EC_s) and deep (0–150 cm) electrical conductivity (EC_d) values. The EC_s data were used as most root activity occurs in the first 50 cm. The final data set consisted of 3386 measurements for EC_s. Figure 11.9 shows the EC_s values, with the green line indicating the division of irrigation sectors. This line separates each variety into different irrigation sectors for IRRIX installation and allows comparison with the application carried out by the farmer. The data obtained with the soil sensor indicate a less variation in soil characteristics between the corresponding irrigation sectors in the zone of the Kay-sweet (red) than between those of the Almaneb (purple) and UFO-4 (brown) varieties.

Sentinel-2 (ESA) satellite images were used to study crop variability. The normalized difference vegetation index (NDVI) values were used to characterize spatial variation within the different varieties and sectors (Fig. 11.10). The maximum

and minimum NDVI values for the different irrigation sectors of the varieties show different values in the sectors for each variety (Table 11.3). In the pre-harvest period, the greatest variability occurred in the Kay-sweet variety.

The soil and crop values indicated that the best location to develop the trial was in the Kay-sweet area because the soil was less variable and crop development was similar, especially in the post-harvest period. The area occupied by the Kay-sweet variety was delimited by a central pipeline controlled by two solenoid valves that allowed two types of irrigation in two zones. In one of the zones (FARMER), traditional irrigation was carried out by the farmer following his experience in irrigation scheduling, replacing ET_c in pre-harvest and a deficit irrigation strategy at 75% of ET_c post-harvest. Irrigation doses were applied using a general irrigation programmer (Agronic 2500, Progrés, Spain) installed on the farm. In the other zone, an IRRIX system was installed to automate irrigation decisions. The IRRIX treatment was applied through the IRRIX application, and the seasonal plan that was introduced in IRRIX was the same as in the FARMER treatment.

11.4.2.2 Automatic Irrigation System

The IRRIX system was calibrated in a national project (RTA2013-00045-C04) funded by the Spanish Agrarian and Food Research Institution (INIA) with different crops. The IRRIX system comprised two components: (a) sensors installed in the field and (b) a cloud-hosted web platform (IRRIX) which uses a control algorithm

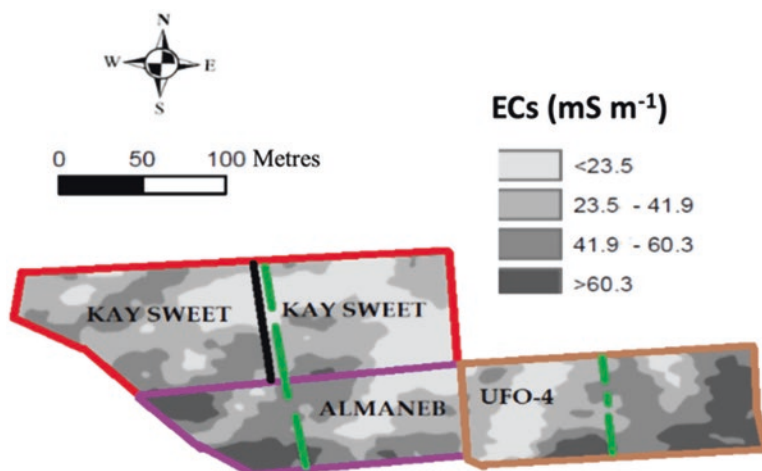


Fig. 11.9 Shallow soil apparent electrical conductivity (EC_s) ($mS\ m^{-1}$) values in trial areas. The dashed green lines indicate the division of irrigation sectors and the continuous red, purple and brown lines indicate the areas corresponding to the different varieties Kay-sweet, Almaneb and UFO-4 varieties, respectively

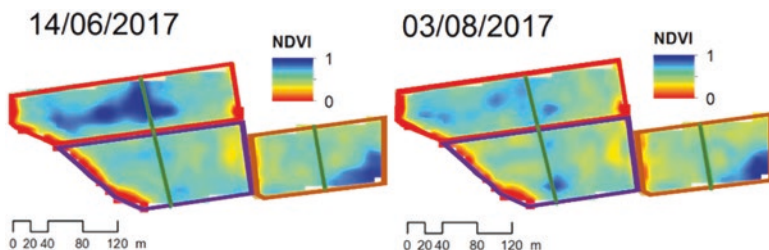


Fig. 11.10 Normalized difference vegetation index (NDVI) values in pre- (14/06/2017) and post-harvest (03/08/2017) periods using Sentinel-2 satellite images of the study zone. The green lines indicate the division of irrigation sectors and the continuous red, purple and brown lines indicate the areas corresponding to the different varieties Kay-sweet, Almaneb and UFO-4 respectively

Table 11.3 Maximum and minimum NDVI values for different varieties in the pre- and post-harvest period

NDVI	Kay-Sweet			Almaneb			UFO-4		
	Min	Max	SD	Min	Max	SD	Min	Max	SD
Pre-harvest	0.50	0.70	0.04	0.49	0.58	0.02	0.47	0.61	0.02
Post-harvest	0.45	0.63	0.02	0.50	0.62	0.03	0.47	0.64	0.03

Min minimum, *Max* maximum, *SD* standard deviation

combines a water-balance-based estimate of crop water needs with readjustment based on sensor readings:

- (a) Various sensors and other devices were installed in the field: (1) Soil moisture sensors at three selected control points (Cp). At each Cp, five 10HS soil moisture sensors (Decagon Devices Inc., Pullman, WA, USA) were installed at different depths and locations in relation to dripper position (two sensors at a depth of 30 cm and located under the dripper; one sensor at a depth of 60 cm and located under the dripper; one sensor at a depth of 30 cm and located between drippers; one sensor at a depth of 60 cm and located between drippers; Fig. 11.11). The 10HS sensors used the general calibration proposed by the manufacturer for mineral soils, (2) an air temperature sensor (CS2015, Campbell Scientific Inc., Logan, UT, US), (3) a solenoid valve, (4) a water meter and (5) a relay. All sensors were connected to a CR1000 data logger (Campbell Scientific Inc., Logan, UT, US). All data were collected every 5 minutes and downloaded to the IRRIX server four times a day.

Other soil moisture measurement points were selected in the farm: (1) Observation points (Op) were also used to monitor soil moisture, but not to control IRRIX. Op1 was installed in the FARMER zone using the Hidrosoph® system with soil moisture sensors every 10 cm to a maximum depth of 80 cm; and (2) Op2 was installed in the IRRIX zone using the same configuration as Cp above.

- (b) A cloud-hosted web platform (IRRIIX) carried out the following daily tasks for water scheduling:

1. Data collection from sensors installed in the field. IRRIX downloads sensor data at periodic intervals during the day. The reference evapotranspiration (ET_0) is estimated daily from the air temperature sensor using the Hargreaves equation (Hargreaves and Allen 2003).
2. Analysis of all data and calculation of irrigation water volumes. The IRRIX analyses all incoming data to detect anomalies and detect if any important event has occurred in the system (irrigation, rain). IRRIX interprets the soil moisture sensors by focusing on the trend, between consecutive days, of the driest measurement of each day (SWCd). Then, to reduce variability between sensors, IRRIX normalizes these values specifically for each sensor through Eq. (11.4).

$$NSWCd = (SWCd - SWCWP) / (SWCFC - SWCWP) \quad (11.4)$$

where soil water content wilting point (SWCWP) and soil water content field capacity (SWCFC) correspond to the values that this sensor would record under wilting point and field capacity conditions, respectively. In practice, the SWCFC is taken at the beginning of the campaign from actual measurements of the system under field conditions, while the value assigned to the SWCWP is the expected SWC value under wilting point conditions for this type of soil. To obtain a single value to summarize the state of an irrigation sector, IRRIX performs a weighted average of the values obtained with the 15 sensors installed in a sector where the weight of each sensor is the product of its reliability and representativeness. The reliability of a sensor is related to the quality of the data that a sensor records, in other words, whether the sensor is operating correctly or not due to some unexpected anomaly. IRRIX automatically estimates sensor reliability on a daily basis with a scale of values ranging from 0 to 1. All sensors have an initial value of 1, and each time an anomaly is detected the reliability value is decreased (multiplied by a value ranging

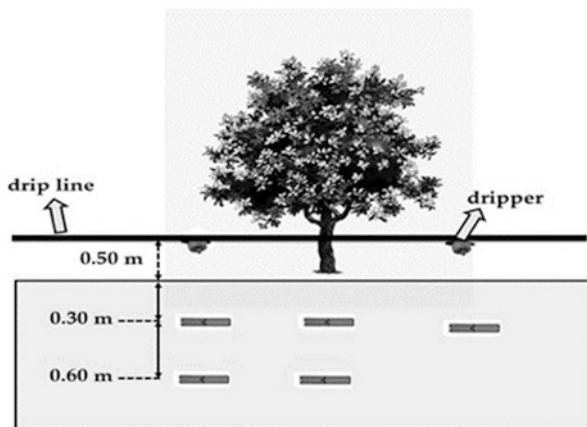


Fig. 11.11 Location of soil moisture sensors

between 0 and 0.5) depending on the seriousness of the anomaly. If the sensor stops working, IRRIX automatically removes it from the system (value of 0) and does not take the data from the sensor into account in its estimates. The representativeness of each sensor refers to whether the information provided by the sensor is relevant or not for the decision-making process in the irrigation control system. The level of representativeness is not set automatically by IRRIX but by the user according to his or her criteria. In practice, representativeness takes the value 1. The automatic system and its control algorithms are described in Millán et al. (2019). Then, IRRIX analyses the set of data to determine and adjust the irrigation dose according to the information provided by the soil sensors.

3. Irrigation scheduling. IRRIX sends the updated irrigation doses to the data logger. Then, the IRRIX system orders the solenoid valve to be opened and closed in order to apply the corresponding irrigation dose as indicated by the water meter.
4. Interaction with users. IRRIX is an autonomous system whose main objective is to free the user from work. The main function of the user is to check that the system has worked correctly, and the irrigation campaign has been undertaken as expected. Any anomaly in the system must also be resolved manually.
5. In addition, before starting the irrigation season, the user must input a seasonal plan to IRRIX that includes a rough forecast of how the water will be distributed throughout the irrigation season. For this purpose, a set of curves has to be defined, and the automated control system positioned between those curves (limits of the system) to ensure it has maximum and minimum cumulative irrigation values. Between these points, IRRIX can modify the irrigation schedule on the basis of the data provided by the soil sensors.

The Cp and Op were located in relation to the soil texture characteristics of the farm. The EC_s map was used to select 46 points to measure the surface (0–30 cm) and deep (30–60 cm) soil properties. Soil sample texture was analyzed using the method introduced by Gee and Bauder (1986). Computation of variograms for ordinary kriging is unreliable with so few data points (Webster and Oliver 1992), therefore, regression kriging with the dense EC_s data was used. Goovaerts and Kerry (2010) showed that the relationship between soil and dense ancillary data can account for a large proportion of the spatial variation and thus, a smaller sample size (around 50 points) can be used when a multi-variate geostatistical approach like regression kriging is used. Regression kriging involves regression between, for example, the sand and EC_s data, computation of a variogram of the residuals and then kriging of the residuals (Millán et al. 2019) (Fig. 11.12). Regression kriging was conducted using the Geostatistical Analyst extension of the ArcGIS software (version 10.3, ESRI, Inc., Redlands, Cal.). The sand and clay content values measured on the map allowed us to identify similar areas between the two zones (Fig. 11.12 a, b). The area next to the dividing line of the sector (black line) was identified as the most representative area for both zones. The three Cps were installed in this area in the IRRIX zone (right-hand side of map), with the distance between the different control points for automatic irrigation limited by the maximum possible cable distance to maintain the electrical signal with sufficient quality. The Op1 was installed in the

FARMER zone (left-hand side of map). Another Op (Op2) was installed in the IRRIX zone to allow monitoring of another point location at the highest elevation for potential pipe leakage problems (Fig. 11.12c), and to carry out checks with respect to the Cp, but becoming part of decision-making process.

Figure 11.13 shows the average soil moisture values at the Cp and Op sites integrated in the root zone (first 60 cm of soil depth). Information from the sensors indicated water application above irrigation needs during the pre-harvest period at all points. This is traditional practice to avoid a loss of fruit size during the pre-harvest period. In this period, the IRRIX system had minor correction limits, determined in the seasonal plan by the farmer, with irrigation doses above crop needs. During the post-harvest period, the farmer uses RDI strategies and so the system limits are larger and allow RDI-based adjustment. With Cp-sourced soil sensor data (Fig. 11.13 a, b, c), the IRRIX management system enabled a significant reduction of irrigation water during the post-harvest period, thereby reducing the large water content in the soil (below the stress line). However, in the case of FARMER management, the decrease was less, resulting, as can be seen in Fig. 11.13e (Op1), in the crop maintaining its water status within the buffer zone of the system (solid and dashed lines). This indicates that the crop was not under the desired stress (dashed line) and that the farmer’s goals were not being achieved during this phase. This was subsequently confirmed with the measured stem water potential values (data not shown). The Op2 (Fig. 11.13d), installed at another point of the IRRIX zone at a

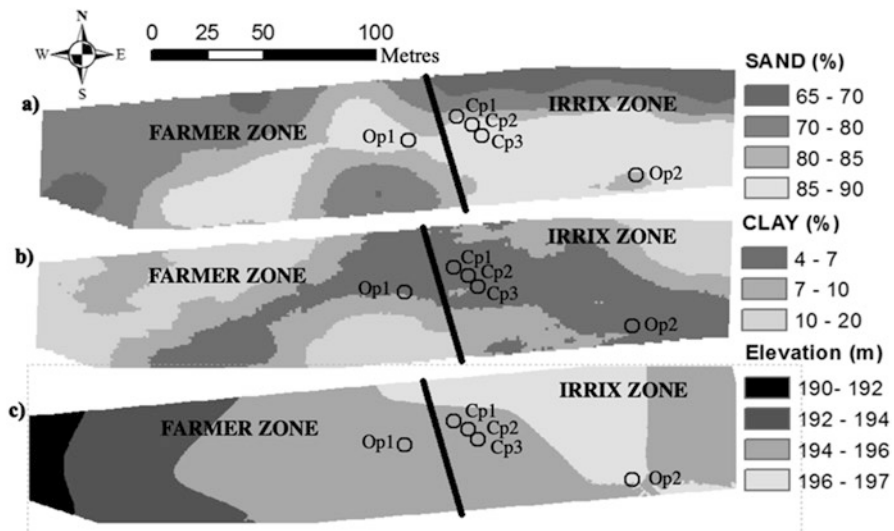


Fig. 11.12 Prediction maps of soil properties (a) sand (%), (b) clay (%) according to the method described by Millan et al. (2020) and elevation (c) elevation (metres) in trial part of the farm. The Cp (control point) and Op (observation point) location shown in the map. The black line is the zone where the sector was divided into farmer and IRRIX zones

higher elevation, showed a lower soil water content (due to different water pressure) closer to the stress situation (dashed line) intended by the farmer.

The IRRIX system not only allowed automation of the irrigation of a commercial plot, but also adjustment of the irrigation dose, reducing the application of water during the post-harvest period and resulting in water savings of 20–25% for all of the irrigation periods (Fig. 11.14a), especially in the post-harvest period. With respect to the impact of the IRRIX strategy on the following year’s yield. The yield was evaluated for 12 trees in each of the zones (FARMER and IRRIX). No losses were observed (Fig 11.14b), with a similar commercial yield between treatments (no significant differences).

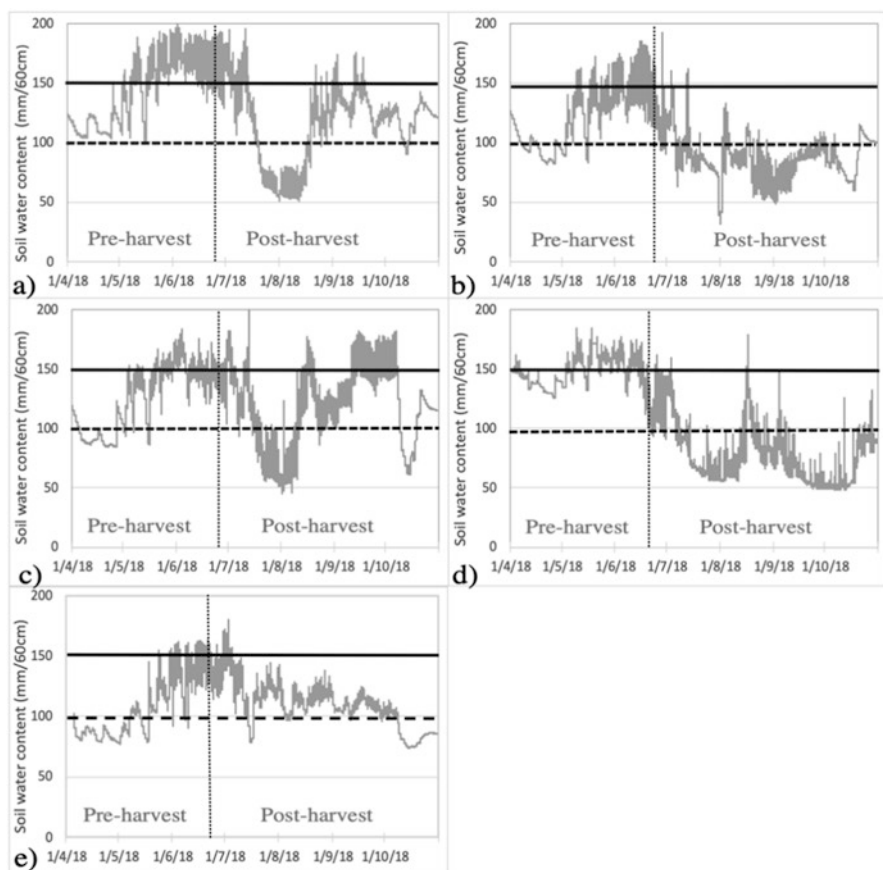


Fig. 11.13 Evolution of soil moisture, average value of sensors in root zone (0–60 cm) at the different control and observation points: Cp1 (a), Cp2 (b), Cp3 (c), Op2 (d) and Op1 (e). Solid line indicates field capacity and dashed line indicates the start of crop stress. The vertical line marks the harvest date

11.4.3 Conclusions

For efficient management of fruit crop irrigation and the possible implementation of water-saving irrigation strategies, soil moisture control systems provide important benefits with knowledge of the amount of water available to the plant in each crop phase; they are cheap, easy-to-install and can measure soil moisture content continuously. However, these systems also have some drawbacks, with the trickiest issues involving sensor positioning, possible errors and inconsistencies in sensor readings, the treatment given to the sensor readings, interpretation of the data obtained and the decision making process. In this sense, advances in computer science combined with the development of ICTs and improvement of communication systems have revolutionized the possibilities for the integration of crop monitoring sensors in DSS. Automatic irrigation systems such as IRRIX allow the integration of DSS with sensors in the field, enabling early estimation of irrigation needs. Having a mechanism of readjustment based on feedback control from soil sensors allows selection of the most reliable data. Such interpretation of the results is very useful for decision making.

The correct installation of the soil moisture sensors in a representative area of the farm is an important factor to obtain useful data for the water management objectives set by the farmer. The use of PA techniques to characterize spatial variation in the soil and plants and selection of the correct zone to install the sensors has also been a major advance. This enables representative data to be obtained of the hydraulic state of the soil that can be applied to the whole plot and helps to avoid irrigation programs that influence each zone in a different way.

The IRRIX system could be very useful to farmers in the application of RDI strategies, saving water and reducing vegetative growth (pruning) while at the same time maintaining yield and fruit quality.

11.5 Conclusions for the Chapter

Three precision irrigation case studies have been described above that address a range of challenges associated with incorporating precision irrigation. The case study from south-eastern USA, presented the use a commercial VRI for pivot irrigation system, the case study from Spain demonstrated an automatic irrigation system for a drip irrigated orchard and the one from Israel described the first steps towards VRDI implementation. Until recently, precision irrigation was based on pre-determined IMZ, essentially based on historical and soil data and predetermined irrigation scheduling based primarily on weather data. Adaptive irrigation control strategies can use both historical data and (near) real-time quantitative measurements of crop status, weather and soil, either singly or in combination, to adjust the irrigation application locally, as required, to account for temporal and spatial variation in the field (McCarthy et al. 2010). All three case studies have shown that

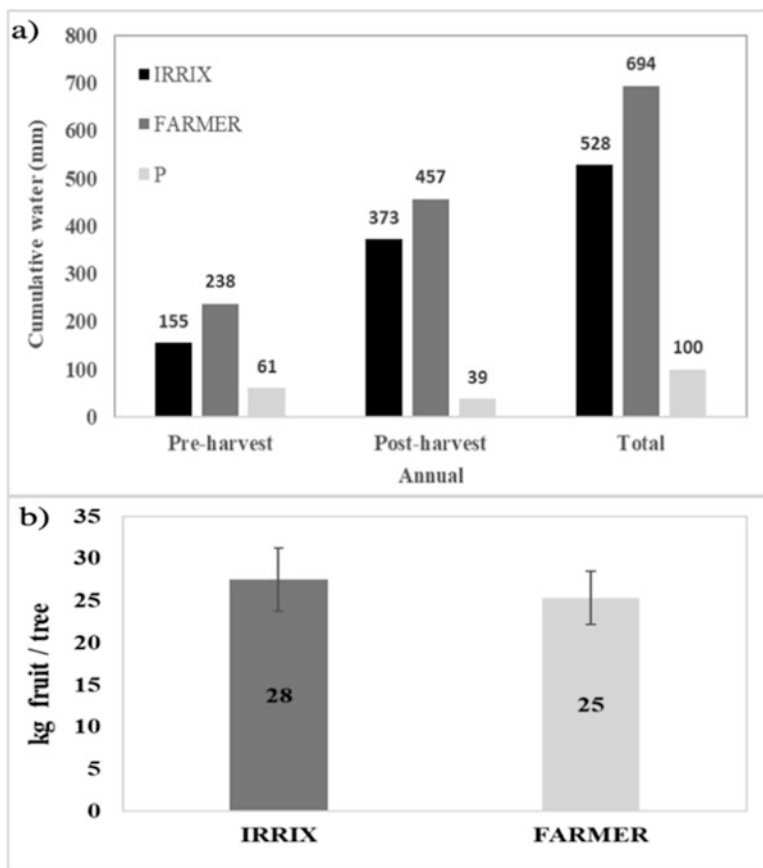


Fig. 11.14 Automatic (IRRIX) and traditional (FARMER) irrigation and rainfall (p) in the different water scheduling programs in pre- and post-harvest period (a) and average yield of 12 trees from each zone in the following growing season (b). The error bars stand for the standard error

timely data provide decision support for VRI management, i.e. soil moisture sensor data (south-eastern USA and Spain) and thermal aerial imagery (Israel). The three cases studies showed that precision irrigation treatments performed better than uniform irrigation. Yield increase was 4.3, 6–15, and 12% in south-eastern USA, Israel and Spain, respectively. In addition, in all cases but one (in Israel, 2018) WUE was improved by 14, 25 and 40% in Israel, Spain and southern USA, respectively.

The reliance on point-sensor data in the case studies from south-eastern USA and Spain dictated the use of pre-determined IMZ, yet, enabled adaptive in-season irrigation management. In-season remotely sensed images can be used further for adaptive IMZ, i.e. to modify their boundaries (Fontanet et al. 2020). The use of satellite imagery and to some extent aerial imagery, however, currently have a relatively long revisit time which limits their use with VRI pivot irrigation systems. Irrigation of a field with VRI pivot irrigation systems is lengthy, thus a snapshot

image does not adequately represent the variation in plant water status that is relevant to irrigation decisions. To overcome that, a sensor network mounted on the lateral of an irrigation system (O'Shaughnessy and Evett 2010) was suggested. The case study from Israel, by comparison showed that remotely sensed imagery might depict the variation in water status well in drip irrigated fields, enabling the delineation of dynamic management zones. In this case, however, the implementation of precision irrigation is limited by the current lack of VRI for drip irrigation. From these case studies, it can be seen that full VRI implementation, which adapts for spatial and temporal changes, faces 'site-specific' challenges, i.e. every irrigation system is unique, and requires unique solutions.

Precision irrigation is studied widely, but is still in its infancy in terms of assimilation and commercialization. Similar to other PA disciplines, PI management is mainly based on: (1) data acquisition mostly from remote and proximal sensing, (2) data processing, (3) modelling and development of spatial decision support systems to manage within-field variability and create prescription maps, and (4) variable-rate application (VRA) devices. Previous scientific efforts regarding PI have concentrated on data acquisition and processing. Until recently, industries have focused mainly on the development of VRI systems. Both scientific and industrial communities currently invest increasing effort to develop advanced decision-making methods and tools (e.g. Navarro-Hellín et al. 2016; McCarthy et al. 2014). More effort should be invested in developing irrigation decision support systems that integrate atmospheric data with timely data from soil sensors and in-season spatial plant data from remote sensing. Moreover, to shift from purely responsive irrigation control that relies on past and 'near real time' soil and plant sensing data, forecasts of soil and plant water status that are based on crop models should also be incorporated into DSS.

References

- Abreu VM, Pereira SL (2002) Sprinkler irrigation systems design using Isadim. St. Joseph, MI, USA
- Alchanatis V, Cohen Y, Cohen S et al (2010) Evaluation of different approaches for estimating and mapping crop water status in cotton with thermal imaging. *Precis Agric* 11(1):27–41
- Allen RG, Pereira L, Raes D et al (1998) Crop evapotranspiration: guidelines for computing crop water requirements: FAO irrigation and drainage paper 56. Rome: Food and Agriculture Organisation
- Bacci L, Battista P, Rapi B (2008) An integrated method for irrigation scheduling of potted plants. *Sci Hortic* 116(1):89–97
- Bahat I, Netzer Y, Ben-Gal A et al (2019) Comparison of water potential and yield parameters under uniform and variable rate drip irrigation in a cabernet sauvignon vineyard. In: Stafford JV (ed) 12th European conference on precision agriculture, Montpellier, France. Wageningen Academic Publishers, pp 125–131
- Cáceres R, Casadesús J, Marfà O (2007) Adaptation of an automatic irrigation-control tray system for outdoor nurseries. *Biosyst Eng* 96(3):419–425
- Casadesús J, Mata M, Marsal J et al (2012) A general algorithm for automated scheduling of drip irrigation in tree crops. *Comput Electron Agric* 83:11–20

- Cohen Y, Alchanatis V, Meron M et al (2005) Estimation of leaf water potential by thermal imagery and spatial analysis. *J Exp Bot* 56(417):1843–1852
- Cohen Y, Alchanatis V, Sela E et al (2015) Crop water status estimation using thermography: multi-year model development using ground-based thermal images. *Precis Agric* 16(3):311–329
- Cohen Y, Agam N, Klapp I et al (2017a) Future approaches to facilitate large-scale adoption of thermal based images as key input in the production of dynamic irrigation management zones. *Adv Anim Biosci* 8(2):546–550
- Cohen Y, Alchanatis V, Saranga Y et al (2017b) Mapping water status based on aerial thermal imagery: comparison of methodologies for upscaling from a single leaf to commercial fields. *Precis Agric* 18(5):801–822
- Davidson JI Jr, Lamb MC, Sternitzke DA (2000) Farm suite-irrigator pro: peanut irrigation software and USER'S guide. The Peanut Foundation, Alexandria
- Evans RG, Sadler EJ (2008) Methods and technologies to improve efficiency of water use. *Water Resour Res* 44(7)
- Fontanet M, Scudiero E, Skaggs TH et al (2020) Dynamic management zones for irrigation scheduling. *Agric Water Manag* 238:106207
- Fridgen JJ, Kitchen NR, Sudduth KA et al (2004) Management zone analyst (Mza). *Agron J* 96(1):100–108
- Gee GW, Bauder JW (1986) Particle-size analysis. In: Klute A (ed) *Methods of soil analysis part 1*. Soil Science Society of America, Madison, pp 383–411
- Gonzalez-Dugo V, Zarco-Tejada P, Nicolas E et al (2013) Using high resolution Uav thermal imagery to assess the variability in the water status of five fruit tree species within a commercial orchard. *Precis Agric* 14(6):660–678
- Goovaerts P, Kerry R (2010) Using ancillary data to improve prediction of soil and crop attributes in precision agriculture. In: Oliver M (ed) *Geostatistical applications for precision agriculture*. Springer, Dordrecht
- Hargreaves GH, Allen RG (2003) History and evaluation of Hargreaves Evapotranspiration Equation. *J Irrigation Drainage Eng* 129(1):53–63
- Hess T (1996) A microcomputer scheduling program for supplementary irrigation. *Comput Electron Agric* 15(3):233–243
- Idso SB, Jackson RD, Pinter PJ Jr et al (1981) Normalizing the stress-degree-day parameter for environmental variability. *Agric Meteorol* 24(C):45–55
- Kim Y, Evans RG (2009) Software design for wireless sensor-based site-specific irrigation. *Comput Electron Agric* 66(2):159–165
- Liakos V, Vellidis G, Tucker M et al (2015) A decision support tool for managing precision irrigation with center pivots. In: Stafford JV (ed) *10th European conference on precision agriculture, Rishon-LeZion, Israel*. Wageningen Academic Publishers, pp 677–683
- Liang X, Liakos V, Wendroth O et al (2016) Scheduling irrigation using an approach based on the Van Genuchten model. *Agric Water Manag* 176:170–179
- Luthra SK, Kaledonkar MJ, Singh OP et al (1997) Design and development of an auto irrigation system. *Agric Water Manag* 33(2):169–181
- McCarthy AC, Hancock NH, Raine SR (2010) Variwise: a general-purpose adaptive control simulation framework for spatially and temporally varied irrigation at sub-field scale. *Comput Electron Agric* 70(1):117–128
- McCarthy AC, Hancock NH, Raine SR (2014) Simulation of irrigation control strategies for cotton using model predictive control within the variwise simulation framework. *Comput Electron Agric* 101:135–147
- McClymont L, Goodwin I, Mazza M et al (2012) Effect of site-specific irrigation management on grapevine yield and fruit quality attributes. *Irrig Sci* 30(6):461–470
- Meeks CD, Snider JL, Porter WM et al (2017) Assessing the utility of primed acclimation for improving water savings in cotton using a sensor-based irrigation scheduling system. *Crop Sci* 57:2117–2129

- Meron M, Grimes DW, Phene CJ et al (1987) Pressure chamber procedures for leaf water potential measurements of cotton. *Irrig Sci* 8(3):215–222
- Meron M, Tsipris J, Orlov V et al (2010) Crop water stress mapping for site-specific irrigation by thermal imagery and artificial reference surfaces. *Precis Agric* 11(2):148–162
- Millán S, Moral FJ, Prieto MH et al (2019) Mapping soil properties and delineating management zones based on electrical conductivity in a hedgerow olive grove. *Trans ASABE* 62(3):749–760
- Millán S, Campillo C, Casadesús J et al (2020) Automatic irrigation scheduling on a hedgerow olive orchard using an algorithm of water balance readjusted with soil moisture sensors. *Sensors (Basel)* 20(9)
- Miranda FR, Yoder RE, Wilkerson JB et al (2005) An autonomous controller for site-specific management of fixed irrigation systems. *Comput Electron Agric* 48(3):183–197
- Möller M, Alchanatis V, Cohen Y et al (2007) Use of thermal and visible imagery for estimating crop water status of irrigated grapevine. *J Exp Bot* 58(4):827–838
- Nadav I, Schweitzer A (2017) Vrđi – variable rate drip irrigation in vineyards. *Adv Anim Biosci* 8(2):569–573
- Navarro-Hellín H, Martínez-del-Rincon J, Domingo-Miguel R et al (2016) A decision support system for managing irrigation in agriculture. *Comput Electron Agric* 124:121–131
- Nolz R, Kammerer G (2017) Evaluating a sensor setup with respect to near-surface soil water monitoring and determination of in-situ water retention functions. *J Hydrol* 549:301–312
- O’Shaughnessy SA, Evett SR (2010) Canopy temperature based system effectively schedules and controls center pivot irrigation of cotton. *Agric Water Manag* 97(9):1310–1316
- O’Shaughnessy SA, Evett SR, Colaizzi PD (2015) Dynamic prescription maps for site-specific variable rate irrigation of cotton. *Agric Water Manag* 159:123–138
- Osroosh Y, Peters RT, Campbell CS et al (2016) Comparison of irrigation automation algorithms for drip-irrigated apple trees. *Comput Electron Agric* 128:87–99
- Perry C, Podcknee S (2003) Development of a variable-rate pivot irrigation control system. In: Georgia water resources conference, The University of Georgia, 23–24 April 2003
- Perry C, Pocknee S., Hansen O, Kvien C, Vellidis G, Hart E. (2002) Development and testing of a variable rate pivot irrigation control system. (ASABE Paper No. 022290). St. Joseph: ASAE
- Peters RT, Evett SR (2008) Automation of a center pivot using the temperature-time-threshold method of irrigation scheduling. *J Irrig Drain Eng* 134(3):286–291
- Romero R, Muriel JL, Garcia I et al (2012) Improving heat-pulse methods to extend the measurement range including reverse flows. In: VIII International symposium on sap flow, Leuven, Belgium, Vol. 951. International Society for Horticultural Science (ISHS), Acta Horticulturae, pp 31–38
- Rosenberg O, Alchanatis V, Cohen Y et al (2014). Are thermal images adequate for irrigation management? In: 12th International Conference on Precision Agriculture, Sacramento, California, USA
- Rud R, Cohen Y, Alchanatis V et al (2014) Crop water stress index derived from multi-year ground and aerial thermal images as an indicator of potato water status. *Precis Agric* 15(3):273–289
- Sanchez LA, Sams B, Alsina MM et al (2017) Improving vineyard water use efficiency and yield with variable rate irrigation in California. *Ad Anim Biosci* 8(2):574–577
- Scudiero E, Teatini P, Manoli G et al (2018) Workflow to establish time-specific zones in precision agriculture by spatiotemporal integration of plant and soil sensing data. *Agronomy* 8(11):253
- Tahar B, Abdellah A, Abdulkhaliq A et al (2011) Evaluation of the effectiveness of an automated irrigation system using wheat crops. *Agric Biol J N Am* 2(1):80–88
- Webster R, Oliver MA (1992) Sample adequately to estimate variograms of soil properties. *J Soil Sci* 43(1):177–192
- Xiang X (2011) Design of fuzzy drip irrigation control system based on Zigbee wireless sensor network. In: Computer and computing technologies in agriculture IV. Berlin Heidelberg: Springer, pp 495–501
- Zhu HL, Li X (2011) Study of automatic control system for irrigation. *Adv Mater Res* 219–220:1463–1467